

Conformational Analysis of Triazine Dendrimers: Using NMR Spectroscopy To Probe the Choreography of a Dendrimer's Dance

Karlos X. Moreno and Eric E. Simanek*

Department of Chemistry, Texas A&M University, MS 3255, College Station, Texas 77843

Received September 25, 2007; Revised Manuscript Received December 17, 2007

ABSTRACT: One-dimensional (1D) and two-dimensional (2D) NMR studies are used to probe the conformation of a melamine dendrimer bearing unique NMR signals from the core to the periphery. Four conceptual anchors for dendrimer conformation emerge from these experiments. First, changes in isomer populations observed by ^1H NMR reveal the onset of globular structure. Second, NOE complexity emerges with globular structure: variable temperature NOESY studies show that the peripheral groups, BOC-protected aliphatic amines, fold back into the globular core of the macromolecule at 75 °C in DMSO- d_6 . Third, variable temperature coefficients measured for NH protons suggest that solvent is largely excluded from the interior of the dendrimer: the carbamate NH groups of the periphery are most sensitive to temperature while the NHs nearest the core show little temperature dependence. Conformation is influenced by solvent choice: backfolding is observed in DMSO- d_6 , but not in either CDCl_3 or CD_3OD . Finally, relaxation studies show that peripheral groups are more dynamic than groups at the core. These anchors consolidate observations made by many groups on disparate systems within a common architecture.

Introduction

Since the first reported synthesis of dendrimers,^{1,2} there have been many efforts to determine the conformation of the macromolecules in solution using both experiment and theory.^{3–34} One of the most straightforward questions to ask is, “where are the groups on the periphery (the so-called surface or end groups)?” Using a self-consistent-field model, de Gennes and Hervet proposed that the dendrimer extends outwardly from the core having all of the end groups on or near the periphery of the molecule (i.e., dense shell).³ In contrast, Lescanec and Muthukumar's simplified kinetic model using a computer simulation of dendritic growth suggested the maximum density is between the assumed dense core and the periphery of the dendrimer as a result of the backfolding of the chain ends.⁴ A more recent self-consistent-field model by Boris and Rubinstein supports the dense core model: density decreased monotonically from the center of the molecule.⁵ Naylor et al. used computer-assisted molecular modeling to infer that as the size increases, the dendrimer's shape progresses from an open structure to a closed spheroid with well-developed cavities and a dense surface.⁶ Monte Carlo calculations performed by Mansfield and Klushin found the chain ends to be distributed throughout the structure and revealed a density maximum midway between the center of mass and the periphery.⁷ Also, using Monte Carlo calculations, Welch and Muthukumar reported that by varying the ionic strength of the solvent, a reversible transition between a dense core and dense shell structure could be achieved.⁸ Molecular dynamics (MD) simulations of dendrimers that incorporate solvent effects have been performed by Murat and Grest.⁹ Their model predicts significant backfolding of the chain ends and a high density area located near the core for all independent of the solvent quality. Their model predicts an overall increase in dendrimer density with decreasing solvent quality. More recently, MD simulations performed in explicit solvent have suggested that dendrimer can backfold in solution.^{10,11} In summary, most of the theoretical studies suggest that backfolding is a common process of dendrimers.

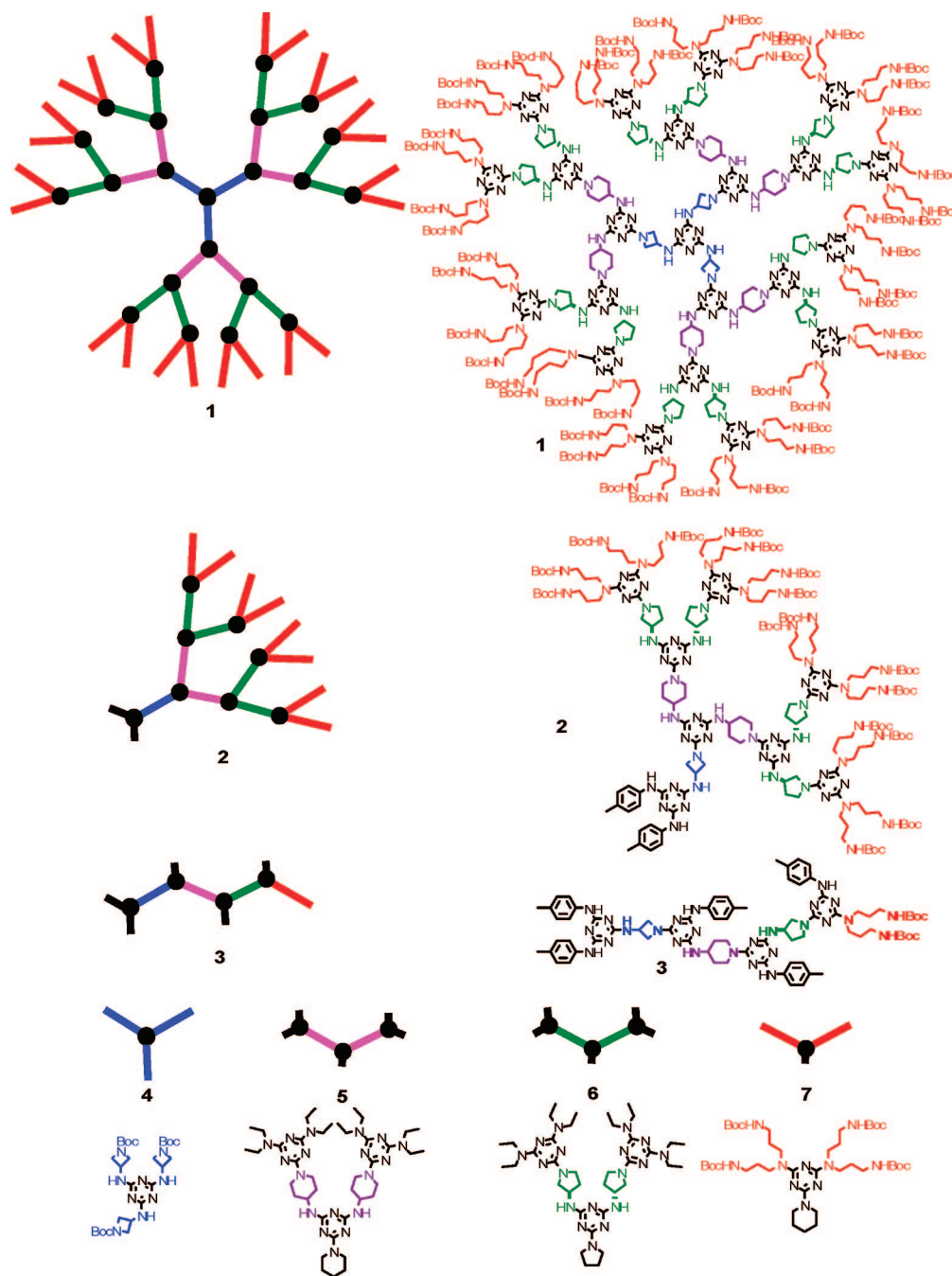
Experimental evidence for backfolding has been obtained using various techniques.^{12–28} In poly(amidoamine) (PAMAM)

dendrimers, Meltzer et al. demonstrated that the chain dynamics did not change dramatically up to the tenth generation using NMR spectroscopy.¹⁵ They conclude that the branches backfold to some extent to relieve steric crowding based on ^2H NMR.¹⁶ More recently, Chen and co-workers demonstrated that, upon changing the pH of the solution, a conformational change can be induced.¹⁷ Unfortunately, the authors could not determine what degree of backfolding, if any, was occurring in their system. In addition to PAMAM dendrimers, polyarylether dendrimers have also been examined. Mourey et al. studied polyaryl ether dendrimers using size exclusion chromatography and differential viscometry.¹⁸ They found that the hydrodynamic radii increased nearly linearly with dendrimer generation and a maximum in the intrinsic viscosity as a function of molecular weight was found. De Backer came to similar conclusions using fluorescence depolarization measurements.¹⁹ Both of these studies are in qualitative agreement with the theoretical study of Lescanec and Muthukumar⁴ in which the end groups can be found throughout the dendrimer volume, i.e., backfolding occurs. Using rotational-echo double-resonance (REDOR) NMR, Woolley et al. were able to show that backfolding occurs in the solid state.²⁰ Additionally, Gorman and co-workers established that the end groups of polyaryl ether dendrimers come in close proximity to the core.²¹ These latter studies were performed using a paramagnetic core and measuring the spin–lattice relaxation (T_1) times of the molecule. Backfolding was attributed to be the major cause of the very rapid electronic energy transfer in polyaryl ether dendrimers.²²

Using viscometry and small-angle neutron-scattering (SANS) measurements of both nitrile- and amine-terminated poly(propyleneimine) (PPI) dendrimers, Scherrenberg et al. found a linear relationship between the radius of the dendrimer and its generation number.²³ This linear relationship was independent of the type of end group or solvent used. These results correlate well with the theoretical results of Murat and Grest,⁹ indicating that PPI dendrimers are flexible with a relatively uniform density distribution resulting from some degree of backfolding. More recently, an extensive SANS study demonstrated that the maximum density is located in the center of the molecule and that the end groups are backfolded.²⁴ The “dendritic box” synthesized by Jansen et al. takes advantage of the end-group

* Corresponding author. E-mail: Simanek@mail.chem.tamu.edu.

Chart 1. Cartoon and Molecular Representation of Dendrimer 1 and Model Compounds Used To Study Its Conformation



backfolding to encapsulate guest molecules.²⁵ Data from X-ray diffraction have provided direct evidence of the end groups backfolding via hydrogen-bond interactions.²⁶ Chai and co-workers performed an extensive NMR study of PPI dendrimers finding evidence for backfolding using 2D nuclear Overhauser effect spectroscopy (NOESY)²⁷ and interactions between chloroform and dendrimer.²⁸ Their results provide further evidence of the flexibility of PPI dendrimers: they observed either a collapsed (backfolded) or extended conformation depending on the solvent used.

The use of NMR spectroscopy to study biomolecules, such as proteins, is a well-established and powerful tool. However, it is difficult to apply these strategies to dendrimers due to the degeneracies of signals resulting from the repetitive nature of the macromolecule. The ability to incorporate unique spectral signatures on the end groups greatly facilitates inquiry into backfolding. Still, size, morphology, and dynamics of dendrimers have been probed

in a limited number of systems. Studying T_1 and spin–spin relaxation (T_2) times of PAMAM dendrimers allowed Meltzer et al. to determine that there is a gradual increase in segment density and that the terminal groups are not densely packed.^{15,16} By studying the ^{13}C T_1 times of a PPI dendrimer with both hydrophilic and hydrophobic end groups, Pan and Ford determined that the conformation may change by varying the solvent.²⁹ Multidimensional NMR techniques have been used to characterize dendrimers, to determine their conformation, and to observe host–guest interactions within them. Chai et al. used 2D and 3D NMR techniques to both characterize and determine the conformation of PPI dendrimers.²⁸ To evaluate host–guest interactions, Morgan et al.,³⁰ Banerjee et al.,³¹ and Broeren et al.³² used 2D NOESY to confirm that the guest molecule was interacting with the dendrimer. To study the secondary interactions of the end groups, VT coefficients and hydrogen/deuterium (H/D) exchange studies have been performed.^{26,33,34}

The goal of these studies are to confirm many of these observations in a single dendrimer system and elaborate on more subtle issues of conformation. We rely on a melamine dendrimer with unique NMR signals from periphery to core to aid our investigations of the conformations of triazine dendrimers. Chart 1 shows the cartoon and chemical structures of the dendrimer and a series of models studied in this report. Details concerning the synthesis and characterization of these materials appear in the Supporting Information.

Results and Discussion

The results and discussion are organized around major lessons learned from these studies. The first lesson learned is that the richness of conformational isomerism (resulting from hindered rotation about the triazine–N bond) gives rise to spectral complexity in the context of signal number, degeneracy, and broad lines. Monitoring this complexity, however, reveals that the distribution of isomers changes as the dendrimer adopts a globular structure. The second lesson learned from nuclear Overhauser effects (NOE) is that signal complexity emerges with globular structure: backfolding and interbranch communication are dependent on size. The third lesson learned is that solvent is largely excluded from the interior of the dendrimer. The fourth lesson learned from relaxation studies is that each “layer” of the dendrimer has different mobility.

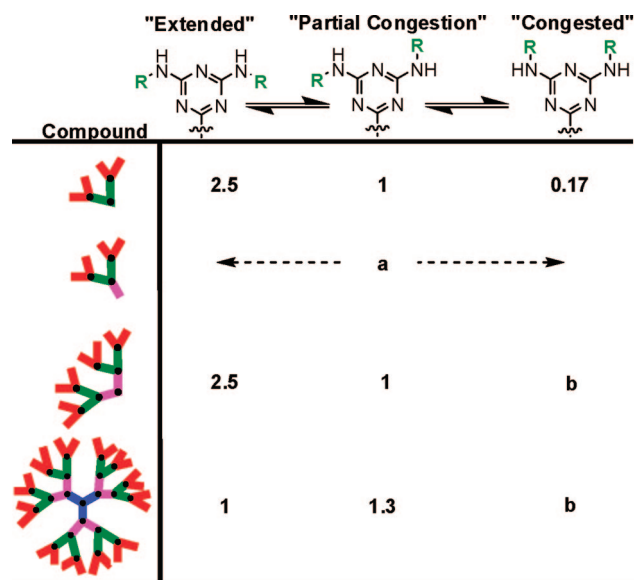
Lesson One. Changes in Isomer Populations Suggest the Onset of Globular Structure. Throughout the dendrimer synthesis, the carbamate NH populations (cis vs trans amides) of the Boc-periphery do not change. The complexity of other regions of the spectra (i.e., the NH region) and broadness observed in many lines suggests that a rich population of rotamers exists. Rotamers derive from hindered rotation about the triazine–exocyclic amine single bond. These rotamers (Scheme 1) place pendent groups in an “extended”, “partially congested”, or “congested” environment. Tentative assignments of these resonances to specific rotamers derives from inferences from simpler models. The Supporting Information provides an extensive discussion of these assignments. The most significant changes in rotamer populations were observed from the pyrrolidine NH populations. These groups are shown in green in Scheme 1. As the synthesis progressed, the population changed from predominantly “extended” architecture attributed to a conformationally less hindered molecule to an architecture that revealed “partial congestion”. Because of broadness of lines, the appearance of “sterically congested” architectures could not be quantified.

Lesson Two: NOE Complexity Emerges with Globular Structure. Figure 1 shows the onset of NOE complexity when comparing the linear model **3** to dendron model **2**, representing 1/3 of the dendrimer, and the entire dendrimer **1**. For clarity, only new NOEs are shown for **2** and **1**.

Model **3** shows simple intra-residue NOES suggesting an open and/or dynamic conformation in solution. The intra-residue NOEs are observed in all architectures, but *only* intra-residue NOEs are seen in model **3**. These NOEs in the azetidine and piperidine rings suggest that ring interconversion may be occurring. If so, these motions are either conserved in the more complex architectures or supplanted by inter-residue NOEs of similar magnitude. The pyrrolidine ring and peripheral groups separately display NOEs between neighboring protons.

Model **2** shows evidence for interbranch communication. In addition to the NOEs observed in **3**, model **2** shows NOEs that can only be explained by the two pyrrolidine rings interacting with each other (Figure 1); specifically, an NOE observed between protons $H_{K'}-H_I$ and H_L-H_I . We do not expect an NOE between these resonances unless there is interbranch

Scheme 1. Effect of Macromolecular Size on Rotamer Population Distribution^a



^a Ratios identify the pyrrolidine (green) NH ratios. (a) Ratio not determined due to overlap with the carbamate moiety (red). (b) Not observed by NMR.

communication or spin diffusion occurring. Spin diffusion may occur in macromolecular systems when $\tau_c \gg \omega_0^{-1}$.³⁵ While this effect can lead to additional cross-peaks observed between all protons within the same spin system, adjusting the mixing time of the NOESY experiment to very short times precludes cross-relaxation steps from occurring, thus eliminating the cross-peak. Decreasing the mixing time of the NOESY experiment from 300 to 50 ms resulted in no noticeable differences in the cross-peaks, thus disfavoring spin diffusion as a possible cause.

Dendrimer **1** provides evidence for both interbranch communication and backfolding of peripheral groups. NOESY experiments were performed at various temperatures (30–75 °C) and concentrations (0.1–10%, w/v) in deuterated dimethyl sulfoxide (DMSO-*d*₆). Figure 2 shows a typical NOESY spectrum of **1** in the range of 1.0–5.0 ppm at 40 °C. Multiple cross-peaks are observed in the spectrum both between different spin systems and the same spin systems. Interactions between the peripheral groups and the pyrrolidine groups are the only interactions between different spin systems, suggesting that the dendrimer end groups are backfolding. Backfolding of the peripheral groups was even observed up to 75 °C. Upon changing the solvent to CDCl₃ or CD₃OD, backfolding was no longer observed. Even small amounts of CD₃OD (<5%) added to DMSO-*d*₆ leads to a disappearance of these NOEs. A possible explanation for this result is that DMSO-*d*₆ does not permeate the dendrimer and only resides outside of the dendrimer molecule, while CDCl₃ or CD₃OD may be able to permeate the dendrimer. While DMSO-*d*₆ would ordinarily be considered a “good solvent” based on similarity in polarity to methanol (dielectric constants, ϵ , for DMSO = 47.2, MeOH = 33, CHCl₃ = 5.5), the most readily identifiable difference to us is the inability of DMSO-*d*₆ to donate a hydrogen bond to the triazine-rich core. When the concentration of the dendrimer was increased from 0.001 to 0.01 M, there was little to no change in chemical shift, potentially supporting that DMSO-*d*₆ resides outside of the dendrimer molecule. With the solvent molecules residing outside of the molecule, this leaves a void within the interior of the dendrimer and the arms are most likely to fold back into the dendrimer. In CDCl₃ or CD₃OD, the arms are most likely in an extended conformation. Rinaldi came to a

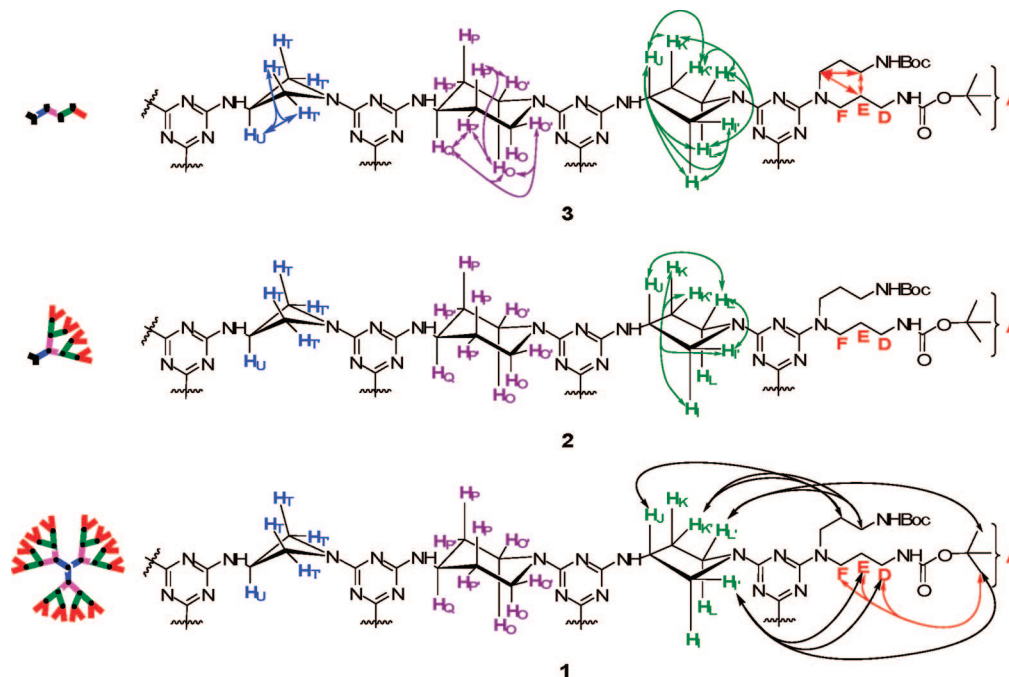


Figure 1. Observed NOEs of models and full dendrimer. Linear model, **3**, shows intraresidue NOEs. Arm model, **2**, identifies additional NOEs not observed in **3**. Dendrimer **1** identifies additional NOEs not observed in **3** or **2**.

Table 1. Variable Temperature Coefficients ($\Delta\delta/\Delta T$, ppb/K) of Dendrimer and Model Compound NHs^{a,b,c}

	NH ^b Conformer	Boc			Pyr		Pip ^c			Az	
		<i>Anti</i>	<i>Syn</i>		(<i>E,E</i>)	(<i>E,Z</i>)	(<i>E,E</i>)	(<i>E,Z</i>)	(<i>Z,Z</i>)		
	1	-6.88	-5.54	-3.54	-7.61	-5.48				-6.16	-5.25
	2	-6.86	-4.27	-3.91	-7.69					-4.46	
	3	-7.36	-5.39	-4.90	-6.63		-8.31			-4.41	
	4									-6.50	-5.24
	5						-8.24	-7.71	-5.10		
	6				-8.47	-5.68					
	7	-6.23	-4.32								

^a All spectra acquired in DMSO-*d*₆. ^b Boc = carbamate NH; Pyr = pyrrolidine NH; Pip = piperidine NH; Az = azetidine NH. ^c Coefficients could not be determined for **1** and **2**.

similar conclusion with PPI dendrimers: backfolding occurred in benzene ($\epsilon = 2.3$) but not chloroform ($\epsilon = 5.5$).²⁸

Lesson Three: Solvent Is Largely Excluded from the Interior of the Dendrimer. Both variable temperature NMR and H/D exchange experiments provide a picture of the role of solvent.

Solvent Shielding Observed in the Dendrimer. Variable temperature NMR studies were used to calculate temperature coefficients ($\Delta\delta/\Delta T$) of the dendrimer and the model compounds to determine whether the NH resonances may be involved in intramolecular hydrogen bonding. Commonly applied to peptides and proteins, it is generally accepted for peptides that if the temperature coefficient is more negative than -4 ppb/K in aqueous solution, the NH is exposed to solvent and not involved in intramolecular hydrogen bonding, while a temperature coefficient less negative than -4 ppb/K is considered to be

involved in intramolecular hydrogen bonding.³⁶ Although dendrimers are considered to be similar in size to proteins, using similar temperature coefficient constraints to evaluate hydrogen bonding of a nonamide NH resonance of our dendrimer in organic solvents may not be accurate. The use of model compounds anchor our interpretation of the magnitude of these values, assuming the NH resonance of the model compound is completely exposed to solvent. These experiments are inherently challenging in that multiple NH lines are observed and the addition of a hydrogen bond donating solvent like deuterated methanol affects the structure of this dendrimer.

Table 1 shows the calculated temperature coefficients of the various NH resonances of the dendrimer and model compounds, **2–7**. The comparison of the NH resonances of dendrimer, **1**, with the respective model (**4–7**) is most useful for us. Differences between these values are evident and support a

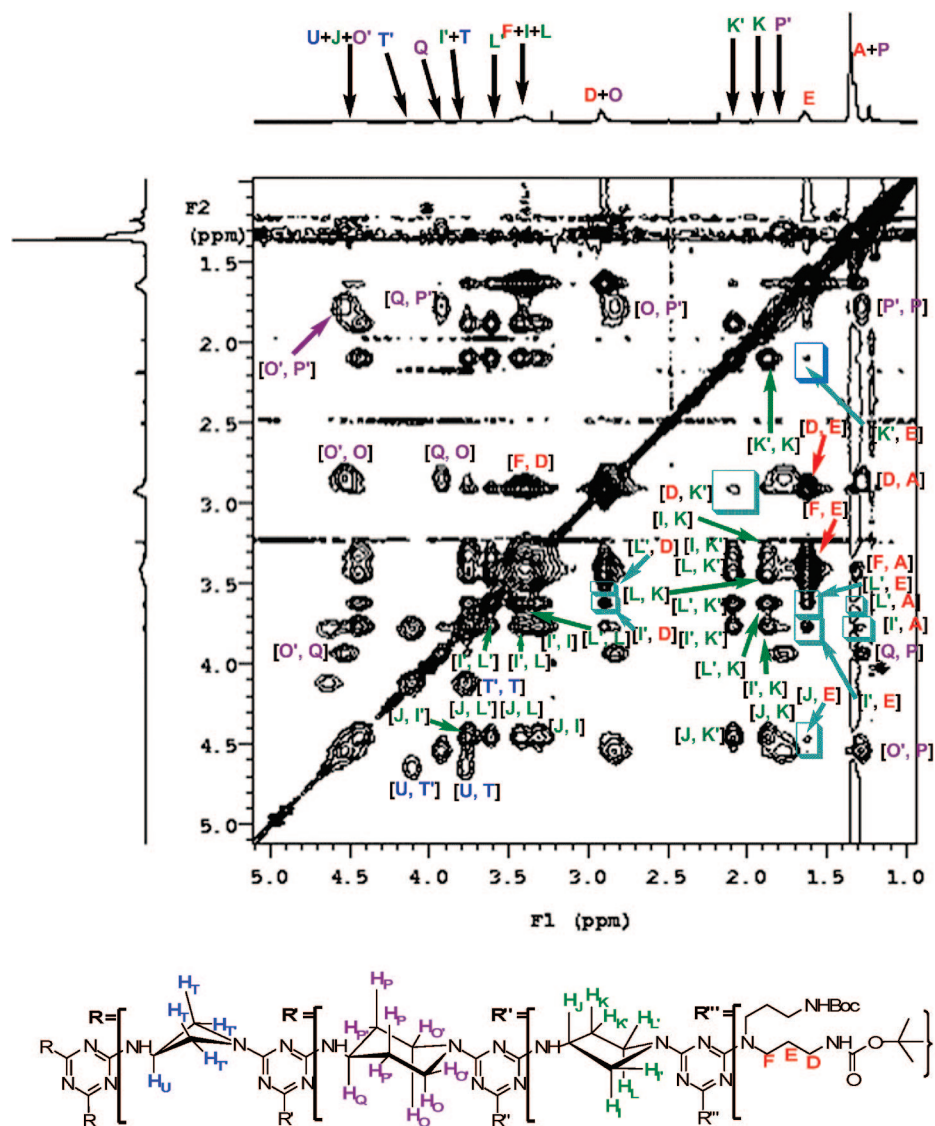


Figure 2. NOESY spectrum of **1** in DMSO- d_6 (2% w/v) at 40 °C. Black boxes identify interactions between different spin systems. Additional cross-peaks are intraspine NOEs caused by interbranch communication or proximity of protons within the linker.

conformation wherein the azetidine, pyrrolidine, and carbamate NH's become less exposed to solvent. Under the current architecture of the dendrimer, the piperidine NH cannot be observed.

Coefficients for the arm (**2**) and linear (**3**) models when compared with model compounds **4–7** echo similar trends, but direct comparisons between these two architectures and the dendrimer are less instructive. For **2**, the NH resonances for the carbamate and pyrrolidine seem to be less exposed to solvent than **1**, while the azetidine NH is even more shielded from solvent. As with the dendrimer, the piperidine NH could not be observed. For **3**, we expected the NH resonances to have similar coefficients as **4–7**, but for the carbamate and pyrrolidine NHs the coefficients have similar values as the dendrimer. The primary anomaly for both models is with the azetidine NH resonance; it is more shielded from the solvent than even the azetidines groups of **1**. Perhaps, the *p*-toluidine groups are somehow prohibiting the NH from interacting with the solvent (no NOEs were observed between the azetidine and *p*-toluidine groups).

H/D Exchange Occurs Rapidly for Azetidine and Pyrrolidine NHs. Hydrogen–deuterium exchange studies can complement the variable temperature studies for identifying whether the NH protons are involved in intramolecular hydrogen-

bonding. Intramolecular hydrogen-bonded NH protons exchange with protic solvents at a much slower rate than NH protons exposed to solvent.³⁷ Preliminary studies with the dendrimer using ^1H NMR suggested that the NH protons of the pyrrolidine and azetidine rings exchange within 2 min, while carbamate NH's did not. Since the piperidine NH protons are buried under the carbamate resonances, no conclusion can be drawn. Direct comparison between different types of exchangeable protons led us to examine the rate of exchange with model compounds **4–7**. For models **4–7**, we observe immediate exchange of the NH protons for **5** and **6** but not for **4** or **7**. The carbamate protons of **7** showed a gradual decrease in signal intensity. The NHs of **4** decreased more rapidly. The “slow” exchange of ^1H for ^2H of the carbamate NHs of the dendrimer, as compared to **5** and **6**, led us to conclude that these protons are involved in intramolecular hydrogen-bonding.

Lesson Four: Each “Layer” of the Dendrimer Has Different Mobility. The mobility of each “layer” is different as judged from spin–lattice relaxation (T_1) and spin–spin relaxation (T_2) studies. In short, spin–lattice relaxation may be used to study intermolecular interactions, while spin–spin relaxation may be used to study intramolecular interactions.³⁵ Figure 3 displays the results of the proton relaxation of our

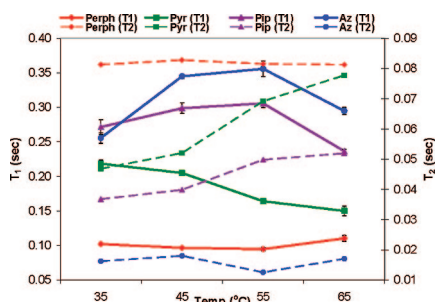


Figure 3. T_1/T_2 vs temperature plot of the various linkers within melamine dendrimer. Solid lines refer to spin–lattice (T_1) relaxation time, and the dashed lines refer to spin–spin (T_2) relaxation time.

dendrimer. The relaxation times depicted here are average values for each linker of the molecule. Evident in both sets of data, we find that each linker exhibits a different relaxation time when compared to the other segments of the dendrimer. The T_1 relaxation values increase from the peripheral groups toward the core of the molecule. For T_2 relaxation, the opposite is true. The peripheral groups have the longest relaxation time. These times decrease as one moves toward the core of the molecule. This suggests that our dendrimer tumbles slowly or in the “slow” regime of the T_1/T_2 vs τ_c , correlation time, curve. The conceptual picture that emerges has the peripheral groups moving more than pyrrolidine segment, which moves more than the piperidine and so on. The data also show that while an increase in temperature also increases the movements of the molecule, the changes are greatest near the outer portions of the molecule. In this study, the relaxation is attributed to dipole–dipole relaxation between two nuclei. Meltzer and Gorman previously concluded that other mechanisms for nuclear relaxation are generally insignificant in solution and where chemically identical but topologically different nuclei are considered.^{15,21}

Conclusion

The result of these studies is a conceptual image of the conformational musings of a third-generation dendrimer based on triazines in DMSO. Evidence from a variety of other, often disparate, studies suggests that this picture may be more general. Our results agree with previously published reports by other groups, such as Lescanec,⁴ Meltzer,^{15,16} Wooley,²⁰ Gorman,²¹ Meijer,^{25,26} and Rinaldi.²⁸ These reports provide evidence for backfolding in different dendrimer systems using different techniques and different dendrimer architectures. Lescanec used computer simulation of dendritic growth to show the chain ends backfold. Meltzer used ^2H NMR and relaxation studies to provide evidence for backfolding in PAMAM dendrimers. Both Wooley and Gorman studied polyaryl ether dendrimers and demonstrated that backfolding occurs using REDOR NMR and relaxation studies, respectively. By using 2D NMR, both Meijer and Rinaldi showed that PPI dendrimers can backfold. Meijer was able to provide crystallographic evidence with a G1 PPI dendrimer. As with our case, Rinaldi showed that the backfolding is a function of solvent. Relaxation studies of PAMAM, PPI, and polyaryl ether dendrimers show that the exterior of the dendrimer has more mobility and the interior of the dendrimer.^{15,16,21,25,28} Our system not only agrees with these studies but also provides evidence that each layer of the dendrimer has different mobilities.

Most useful to us is to draw an analogy. In consideration of any number of classical dances—the waltz, tango, foxtrot, or chicken—we are inclined to pick the Macarena as most representative of the motions of triazine dendrimers in DMSO- d_6 . A richness in rotational isomers exist on the NMR time scale. Groups on the periphery fold back toward the dendrimer’s core.

Similarly, in accordance with relaxation studies, these peripheral groups move more rapidly than groups closer to the interior. Finally, relaxation appears to be manifest primarily by these movements and less so by tumbling events. The lack of concentration dependence on these events suggests that the molecule dances alone and not in concert with other molecules. Finally, this molecular dance is dependent on the solvent, changing the solvent to chloroform or methanol leads to a different conformation.

Acknowledgment. This work was supported by the National Institutes of Health (NIGMS 65460). K.X.M. thanks the NSF for a predoctoral award through the GK-12 program.

Supporting Information Available: Description of materials, instrumentation, and full synthetic and NMR procedures. This material is available free of charge via the Internet at <http://pubs.acs.org>.

References and Notes

- (1) Tomalia, D. A.; Baker, H.; Dewald, J.; Hall, M.; Kallos, G.; Martin, S.; Roeck, J.; Ryder, J.; Smith, P. *Polym. J. (Tokyo)* **1985**, *17*, 117–132.
- (2) Hawker, C. J.; Fréchet, J. M. J. *J. Am. Chem. Soc.* **1990**, *112*, 7638–7647.
- (3) de Gennes, P. G.; Hervet, H. *J. Phys. Lett. Paris* **1983**, *44*, 351–360.
- (4) Lescanec, R. L.; Muthukumar, M. *Macromolecules* **1990**, *23*, 2280–2288.
- (5) Boris, D.; Rubinstein, M. *Macromolecules* **1996**, *29*, 7251–7260.
- (6) Naylor, A. M.; Goddard, W. A., III; Kiefer, G. E.; Tomalia, D. A. *J. Am. Chem. Soc.* **1989**, *111*, 2339–2341.
- (7) Mansfield, M. L.; Klushin, L. I. *Macromolecules* **1993**, *26*, 4262–4268.
- (8) Welch, P.; Muthukumar, M. *Macromolecules* **1998**, *31*, 5892–5897.
- (9) Murat, M.; Grest, G. S. *Macromolecules* **1996**, *29*, 1278–1285.
- (10) Karatasos, K.; Adolf, D. B.; Davies, G. R. *J. Chem. Phys.* **2001**, *115*, 5310–5318.
- (11) Suek, N. W.; Lamm, M. H. *Macromolecules* **2006**, *39*, 4247–4255.
- (12) Bosman, A. W.; Janssen, H. M.; Meijer, E. W.; *Chem. Rev.* **1999**, *99*, 1665–1688 and references therein.
- (13) Peerlings, H. W. I.; Trimbach, D. C.; Meijer, E. W. *Chem. Commun.* **1998**, *4*, 497–498.
- (14) Rosini, C.; Superchi, S.; Peerlings, H. W. I.; Meijer, E. W. *Eur. J. Org. Chem.* **2000**, *1*, 61–71.
- (15) Meltzer, A. D.; Tirrell, D. A.; Jones, A. A.; Inglefield, P. T.; Hedstrand, D. M.; Tomalia, D. A. *Macromolecules* **1992**, *25*, 4541–4548.
- (16) Meltzer, A. D.; Tirrell, D. A.; Jones, A. A.; Inglefield, P. T. *Macromolecules* **1992**, *25*, 4549–4552.
- (17) Chen, W.; Tomalia, D. A.; Thomas, J. L. *Macromolecules* **2000**, *33*, 9169–9172.
- (18) Mourey, T. H.; Turner, S. R.; Rubinstein, M.; Fréchet, J. M. J.; Hawker, C. J.; Wooley, K. L. *Macromolecules* **1992**, *25*, 2401–2406.
- (19) De Backer, S.; Prinzie, Y.; Veheijen, W.; Smet, M.; Desmedt, K.; Dehaen, W.; De Schryver, F. C. *J. Phys. Chem. A* **1998**, *102*, 5451–5455.
- (20) Wooley, K. L.; Klug, C. A.; Tasaki, K.; Schaefer, J. *J. Am. Chem. Soc.* **1997**, *119*, 53–58.
- (21) Gorman, C. B.; Hager, M. W.; Parkhurst, B. L.; Smith, J. C. *Macromolecules* **1998**, *31*, 815–828.
- (22) Thomas, K. R. J.; Thompson, A. L.; Sivakumar, A. V.; Bardeen, C. J.; Thayumanavan, S. *J. Am. Chem. Soc.* **2005**, *127*, 373–383.
- (23) Scherrenberg, R.; Coussens, B.; van Vliet, P.; Edouard, G.; Brackman, J.; de Brabander, E.; Mortensen, K. *Macromolecules* **1998**, *31*, 456–461.
- (24) Rosenfeldt, S.; Dingenouts, N.; Ballauff, M.; Werner, N.; Vogtle, F.; Lindner, P. *Macromolecules* **2002**, *35*, 8098–8105.
- (25) Jansen, J. F. G. A.; de Barbender-van den Berg, E. M. M.; Meijer, E. W. *Science* **1994**, *266*, 1226–29.
- (26) Bosman, A. W.; Bruining, M. J.; Kooijman, H.; Spek, A. L.; Janssen, R. A. J.; Meijer, E. W. *J. Am. Chem. Soc.* **1998**, *120*, 8547–8548.
- (27) Jeener, J.; Meier, B. H.; Bachmann, P.; Ernst, R. R. *J. Chem. Phys.* **1979**, *71*, 4546–4553.

- (28) Chai, M.; Niu, Y.; Youngs, W. J.; Rinaldi, P. L. *J. Am. Chem. Soc.* **2001**, *123*, 4670–4678.
- (29) Pan, Y.; Ford, W. T. *Macromolecules* **2000**, *33*, 3731–3738.
- (30) Morgan, M. T.; Carnahan, M. A.; Immoos, C. E.; Ribiero, A. A.; Finkelstein, S.; Lee, S. J.; Grinstaff, M. W. *J. Am. Chem. Soc.* **2003**, *125*, 15485–15489.
- (31) Banerjee, D.; Broeren, M. A. C.; van Genderen, M. H. P.; Meijer, E. W.; Rinaldi, P. L. *Macromolecules* **2004**, *37*, 8313–8318.
- (32) Broeren, M. A. C.; de Waal, B. F. M.; van Genderen, M. H. P.; Sanders, H. M. H. F.; Fytas, G.; Meijer, E. W. *J. Am. Chem. Soc.* **2005**, *127*, 10334–10343.
- (33) Mong, T. K.-K.; Niu, A.; Chow, H.-F.; Wu, C.; Li, L.; Chen, R. *Chem.—Eur. J.* **2001**, *7*, 686–699.
- (34) Appoh, F. E.; Thomas, D. S.; Kraatz, H.-B. *Macromolecules* **2005**, *38*, 7562–7570.
- (35) Wuthrich, K. *NMR of Proteins and Nucleic Acids*; John Wiley & Sons: New York, 1986; pp 97–98.
- (36) Kessler, H. *Angew. Chem., Int. Ed. Engl.* **1982**, *21*, 512–523.
- (37) Lenormant, H.; Blout, E. R. *Nature (London)* **1953**, *172*, 770–771.

MA702143F